SLAC–PUB–5300
July 1990
T

Causality Between Conducting Plates*

SHAHAR BEN-MENAHEM

Stanford Linear Accelerator Center
Stanford University, Stanford, California 94309

ABSTRACT

A two-loop QED effect, uncovered by Scharnhorst, causes the phase and group velocities of an electromagnetic wave with $\omega << m_e$ to slightly exceed c, when the wave is travelling in vacuo between, and perpendicular to, two parallel conducting plates. Using *causal* rather than Feynman graphs, we show that the wavefront still travels at exactly c. The two-loop effect thus poses no threat to causality in QED.

Submitted to *Phys. Lett.* **B**

⋆ Work supported by the Department of Energy, contract DE-AC03-76SF00515.

1. Introduction

It has recently been claimed[1,2] that a two-loop effect in QED gives rise to the propagation of some electromagnetic signals at a speed exceeding c, in a vacuum between two parallel, perfectly conducting plates. Scharnhorst[1] finds that at low frequencies ($\omega << m_e$), electromagnetic waves travelling at right angle to the plates have a *phase velocity* exceeding c (the speed of light in vacuo). Since dispersion is negligible for that range of frequencies, he correctly states that the *group velocity* also exceeds c in this situation. However, the implication (made explicit in ref. 2) that *signals* can therefore be sent at speeds greater than c, is incorrect, as we demonstrate in this note. Thus the two-loop effect of ref.1 does not affect causality in QED.

Our approach shall be two-pronged: we first explain (section 2) how high-frequency effects render the low-ω results of ref.1 irrelevant for signal propagation. We then outline in sections 3-4 the proof that, at least in two-loop perturbation theory, the wavefronts of electromagnetic signals between the plates must travel at exactly the speed c. This is done using a manifestly causal diagrammatic expansion for the photon-photon commutator. Since causality is formally manifest in this approach, the task of proving it consists merely of verifying gauge invariance, and then using it to show that the plates do not modify the leading light-cone singularity of the photon-photon commutator. These techniques most likely follow through to all orders in perturbation theory, and in any renormalizable field theory subject to any (non-gravitational!) external fields or boundary conditions.

We note in passing that the plate boundary conditions are highly idealized, and are perhaps unrealistic even for the purpose of studying causal propagation far from the plates; but causality is safe even with the idealized boundary conditions.

Before embarking on our detailed arguments, it is worthwhile to point out that there is no obstacle to effects of the plates on truly low-energy physics, for example the effective mass and magnetic moment of the electron[3,4] .

2. High Frequency Effects

We begin by reviewing the results of ref. 1. Let the plates be the infinite planes $x_3 = 0$ and $x_3 = L$, where $L >> m^{-1}$, $m = m_e$ being the electron mass. We work in natural units, $c = \hbar = 1^\star$.

The plates are assumed perfectly conducting, so their only effect on the photon fields between them is to impose the boundary conditions

$$E_1 = E_2 = B_3 = 0 \quad at \quad x_3 = 0,\ L, \tag{1}$$

with $\mathbf{E}, \mathbf{B}$ the electric and magnetic fields, respectively. No boundary conditions are imposed on the electron field ψ, since its propagator is short-range relative to L, and we are only interested in the propagation of signals which are emitted and detected many compton wavelengths away from either plate. By analyzing the low-frequency quantum effective action in the photon sector, it is found that the dispersion relation in the regime $\frac{1}{L} << \omega << m_e$ is[1][2]

$$\omega^2 \approx k_1^2 + k_2^2 + \frac{1}{n_\perp^2} k_3^2, \quad n_\perp < 1, \tag{2}$$

where it is assumed that the wave propagation is studied at a position x_3 satisfying $m x_3 >> 1$, $m(L - x_3) >> 1^\dagger$.

The expression for $n_\perp$ is [1]

$$n_\perp = 1 - \zeta \frac{e^4}{(mL)^4} \tag{3}$$

where ζ is a pure number and e the electron charge. The Feynman diagrams contributing to this effect are shown in fig. 1.

$\star$ We employ the metric $\eta_{\mu\nu} = (+,-,-,-)$, and denote spatial vectors by boldface letters. We also denote: $\partial_\mu^x = \partial/\partial x^\mu$, $(\partial^2)^x = \partial_\mu^x \partial^{x\mu}$, and $\nabla^2 = \partial_i \partial_i$.

$\dagger$ The corrections to eq.(2) depend on x_3, so this dispersion relation should be understood in the WKB sense.

Now, in order to exploit eq.(2) for sending faster-than-c signals, we assemble a wave packet travelling, on the average, along the 3 axis. Since we do not wish the neglected dispersive terms in eq.(2) to rear their ugly head, the wavefront of the packet cannot be a step function — it must be smeared on the scale of the compton wavelength $1/m$. Thus, to violate causality, the wavefront must, at some time after its formation, move beyond the light cone by a distance δx larger than $1/m$. Hence, if a measurement of $\mathbf{E}$ or $\mathbf{B}$ is performed a time t after the creation of the packet, we inquire whether in

$$\delta x \approx (\frac{1}{n_\perp} - 1)t \approx \zeta \frac{e^4}{(mL)^4} t > \frac{1}{m}. \tag{4}$$

it is possible to satisfy the rightmost inequality. But on the other hand, t must not exceed L, or else the original and reflected waves will permeate the entire region between the plates‡. So we must restrict to $t < L$, which is inconsistent with eq.(4), as $L >> m^{-1}$ by assumption. Therefore, in order to observe faster-than-c propagation of the wavefront, it is necessary to sharpen the falloff of the fields at the wavefront to a length scale less than $1/m$. This feat requires the inclusion in the packet of waves with $\omega > m$, for which eq.(3) is a bad approximation. Thus, high-frequency dispersion invalidates the application of the Scharnhorst effect to sending signals faster than c.

‡ this is true if the packet is a plane wave, localized only in the 3 direction. In the more realistic case that it is also localized in the 1,2 directions, then at $t > L$, due to reflections, its wavefront is travelling on the average in directions *parallel* to the plates, and thus no violations of causality are expected from eq.(2).

3. Commutator Functions.

At the level of quantum fields, the question of causality is properly investigated through commutators of fields. Let us quantize QED between the plates in the Coulomb gauge, subject to eq.(1). We turn on a weak external current $J_\mu(y)$, localized in space and time, and then measure the expectation values $\langle \mathbf{E}(x)\rangle$, $\langle \mathbf{B}(x)\rangle$ in the vacuum state between the plates. The response functions[§]

$$\frac{\delta}{\delta J_\mu(y)}\langle E_i(x)\rangle, \quad \frac{\delta}{\delta J_\mu(y)}\langle B_i(x)\rangle \tag{5}$$

are essentially the vacuum expectation values of commutators of $\mathbf{E}(x)$, $\mathbf{B}(x)$ with the fields at y. These response functions (referred to hereafter as *commutator functions*) contain the information on photon causal propagation. Wavefronts cannot exceed c if, and only if, these functions vanish identically outside the light cone ($(x-y)^2 < 0$). For simplicity, we concentrate on the magnetic commutator function

$$\frac{\delta}{\delta J_j(y)}\langle B_i(x)\rangle,$$

which for a free electromagnetic field between the plates, is

$$\frac{\delta}{\delta J_j(y)}\langle B_i^{(0)}(x)\rangle = \epsilon_{ikj}\partial_k^x G_r^{(0)}(x,y). \tag{6}$$

Here the 0 superscript denotes a free field, and $G_r^{(0)}$ is the free massless scalar retarded Green's function, subject to the plate boundary conditions:

$$\left.\begin{aligned}(\partial^2)^x G_r^{(0)}(x,y) =& \delta^{(4)}(x-y),\\ G_r^{(0)}(x,y) =& 0 \quad if \quad x_3 = 0,\ L \quad or \quad y_3 = 0,\ L.\end{aligned}\right\} \tag{7}$$

§ All variations w.r.t. J are evaluated at $J = 0$.

Denote by $\hat{G}_r^{(0)}(x-y)$ the same object in infinite space,

$$\hat{G}_r^{(0)}(x) = -\int \frac{d^4k}{(2\pi)^4} \frac{1}{k^2 + i\epsilon k_0} e^{-ik\cdot x} = \frac{1}{4\pi|\mathbf{x}|}\theta(x_0)\delta(x_0 - |\mathbf{x}|). \tag{8}$$

Then by the method of images,

$$\left.\begin{aligned} G_r^{(0)}(x,y) = \sum_{n=-\infty}^{\infty} \big(\hat{G}_r^{(0)}(x_\mu - y_\mu, x_3 - y_3 + 2nL) \\ -\hat{G}_r^{(0)}(x_\mu - y_\mu, x_3 + y_3 + 2nL)\big) \\ = \hat{G}_r^{(0)}(x-y) + \quad reflections \end{aligned}\right\} \tag{9}$$

with μ ranging over 0,1,2. Since $\hat{G}_r^{(0)}$ is causal, then clearly so are the reflection terms in eq.(9)¶.

Since we intend to treat the commutator functions perturbatively, it is insufficient to show that, order by order, these functions vanish outside the light cone. One must show that their leading singularity structure *on* the light cone (namely eq.(8)) is unaffected by the plates. In the free-field case, this follows at once from eq.(9), since the reflection terms vanish on the light cone (assuming $\mathbf{x}$ and $\mathbf{y}$ are not on the plates). Had it not been for the dispersive corrections to eq.(2), the light cone would be 'tilted' because of the $1/n_\perp^2$ factor and, to order e^4, the commutator function would have received a correction in which $\delta(x_0 - |\mathbf{x}|)$ is replaced by a *derivative* of a delta function. but we shall see that the plates cannot, in fact, affect the leading light-cone singularity structure*, and thus the wavefront of a localized disturbance moves at precisely the speed c.

¶ The more familiar expression for $G_r^{(0)}$ as a sum over cavity modes, is related to eq.(9) via a Poisson resummation.

* Note, however, that perturbative corrections (not related specifically to the boundaries) *do* modify the free light-cone singularity logarithmically.

4. Causal Graphs.

We wish to find the perturbative QED corrections to eq.(6). The most natural way to accomplish this is by iteratively solving the field equations for the Heisenberg field operators, in the presence of the conserved external source J_i (J_0=0). This is essentially the approach used by Yang and Feldman[5]. The equations are**

$$\psi(x) = \psi^{(0)}(x) + (-i\,\partial\!\!\!/^x - m)\hat{G}_r^{(0)}(x-y;m)e A\!\!\!/(y)\psi(y), \tag{10}$$

$$\bar{\psi}(x) = \bar{\psi}^{(0)}(x) + \bar{\psi}(y)A\!\!\!/(y)(-i\,\partial\!\!\!/^y - m)\hat{G}_r^{(0)}(y-x;m), \tag{11}$$

$$A_0(x) = -\left(\frac{1}{\nabla^2}\right)_{xy} e\!:\!\bar{\psi}(y)\gamma_0\psi(y)\!:, \tag{12}$$

$$A_i(x) = A_i^{(0)}(x) + G_r^{(0)}(x,y)\left(\delta_{ij} - \frac{\partial_i\partial_j}{\nabla^2}\right)_{yz}(e\bar{\psi}(z)\gamma_j\psi(z) + J_j(z)) \tag{13}$$

where: zero superscripts refer to free fields between the plates, summation over repeated indices is implied, and spacetime labels are treated as indices. $\hat{G}_r^{(0)}(x;m)$ is defined as in eq.(8), but with a mass m,

$$\hat{G}_r^{(0)}(x;m) = -\int \frac{d^4k}{(2\pi)^4} e^{-ik\cdot x} \frac{1}{k^2 - m^2 + i\epsilon k_0}, \tag{14}$$

whereas $\hat{G}_a^{(0)}$ is the corresponding *advanced* Green's function:

$$\hat{G}_a^{(0)}(x;m) = -\int \frac{d^4k}{(2\pi)^4} e^{-ik\cdot x} \frac{1}{k^2 - m^2 - i\epsilon k_0}. \tag{15}$$

The two electron Green's functions appearing in eqs.(10)-(11) are thus, in momen-

---

** A comment concerning the operator ordering in eqs. (10)-(13). Any operator ordering for the field bilinears would give the same physical results, except that the free vacuum expectation of $\bar{\psi}\gamma^0\psi$ should be subtracted from the charge density operator (this is what we mean by the normal-ordering notation in eq.(12).). A change of ordering in the product $A\!\!\!/\psi$ merely adds a divergent counterterm to the electron's mass. But this insensitivity to ordering is a result of the equal-time canonical commutation relations of the interacting fields. In a Lorentz invariant vacuum, the CCR imply full causality. In the presence of the plates, however, the CCR are a weaker assumption than causality. Thus, completeness would require verifying causality for all possible (consistent) orderings. We shall stick with the ordering - indicated in eqs.(10)-(13). Formally, of course, the interacting CCR are guaranteed, since the interactions change the fields by a canonical transformation.

tum space, $(\not k + m)/(k^2 - m^2 \pm i\epsilon k_0)$, with the $(+,\ -)$ signs corresponding to retarded and advanced functions, respectively. $(-i\ \not\partial - m)\hat{G}_a^{(0)}$ appears because it is the *positron's* retarded Green's function. We make use of the residual gauge freedom to choose the boundary conditions $A_\mu = 0$ at the plates, which defines $1/\nabla^2$.

We may now use eqs. (10)-(13) to evaluate the commutator functions. As in section 3, we concentrate for concreteness on $\frac{\delta}{\delta J_j(y)}\langle B_i(x)\rangle$. It consists of a series of *causal graphs.* These are like Feynman graphs, except that each Feynman graph (in this case, for the photon propagator) is replaced by a sum of several causal graphs. This proliferation comes about because there are several kinds of electron (or photon) propagators appearing in the new expansion. The electron propagators appearing are retarded, advanced or 'on shell' – the latter is

$$-i\langle\bar{\psi}^{(0)}(y)\psi^{(0)}(x)\rangle = \int \frac{d^4k}{(2\pi)^4}(\not k + m)2\pi i\theta(-k_0)\delta(k^2 - m^2)e^{-ik\cdot(x-y)} \qquad (16)$$

and is really not a propagator, but rather a polarization sum over all the on-shell electron states. By abuse of language, we shall refer to it as an on-shell propagator.

Thus there are three types of electron propagators in causal graphs. The photon has three as well: the retarded $G_r^{(0)}(x,y)(\delta_{ij} - \partial_i\partial_j/\nabla^2)$, the Coulomb $(-1/\nabla^2)$ and the on-shell $i\langle A_i^{(0)}(x)A_j^{(0)}(y)\rangle$. Some one- and two-loop causal graphs contributing to the commutator function are shown in Fig.2***.

Had this expansion been carried out in a non-gauge field theory, the free propagators which appear explicitly in eqs.(10)-(13) would be both retarded and causal. Any causal graph contributing to a commutator function of the points x and y

*** The two one-loop graphs $2a$, $2b$ are related by charge conjugation and are thus identical in value. Note that charge conjugation always exchanges the 'a' and 'r' labels, and reverses the arrows in electron propagators (see caption for Figs.2). Of the photon propagators, only the on-shell variety is affected, its arrow being reversed. That these are the effects of charge conjugation is not immediately evident, but can be proven from eqs.(10)-(13), by a. reversing the order of ψ and $\bar{\psi}$ in eqs.(12)-(13) (which costs a minus sign) and b. interchanging ψ and $\bar{\psi}$ everywhere using the usual charge-conjugation operation.

would then contain at least one unbroken chain of causal Green's functions, running forward in time from the source point y to the measurement point x. The other propagators, which may be either retarded, advanced or on-shell, result from contractions of the sourceless, interacting fields with one another when the expectation value is taken.

In Coulomb-gauge QED, however, the ubiquitous $1/\nabla^2$ is noncausal. But in Feynman graphs, it is known that their contributions to any scattering process cancel[6] . For causal graphs, the cancellation follows through using the same techniques, based on the Ward identity. The only new ingredient here is that on-shell propagators qualify as a pair of external electrons, one incoming and the other outgoing.

Thus gauge invariance allows us to unify $G_r^{(0)}(\delta_{ij} - \partial_i\partial_j/\nabla^2)$ and $(-1/\nabla^2)$ into a retarded, causal, Feynman-gauge Green's function, $-G_r^{(0)}\eta_{\mu\nu}$. The on-shell photon propagator retains the inverse laplacian, and is

$$i\langle A_i^{(0)}(x)A_j^{(0)}(y)\rangle = (\delta_{ij} - \frac{\partial_i\partial_j}{\nabla^2})\int\frac{d^4k}{(2\pi)^4}2\pi i\theta(k_0)\delta(k^2)e^{ik\cdot(x-y)} + \quad reflections \tag{17}$$

The presence of $\frac{1}{\nabla^2}$ here is not a problem, since on-shell propagators are in any case noncausal and are not required to complete the causal chain, as the graphs in fig.2 exemplify. Nevertheless, by again utilizing gauge invariance, eq.(17) may be replaced by the covariant Feynman-gauge expression

$$-\eta_{\mu\nu}\int\frac{d^4k}{(2\pi)^4}2\pi i\theta(k_0)\delta(k^2)e^{ik\cdot(x-y)} + \quad reflections. \tag{18}$$

To all orders in the causal expansion, one has for the magnetic commutator function:

$$\frac{\delta}{\delta J_j(y)}\langle B_i(x)\rangle = \epsilon_{ikl}\partial_k^x\{\delta_{lj}G_r^{(0)}(x,y) + G_r^{(0)}(x,z)\Sigma_{l\mu}(z,w)\frac{\delta}{\delta J_j(y)}\langle A^\mu(w)\rangle\}, \tag{19}$$

where Σ is a sum of one-particle- irreducible causal graphs. A similar equation holds for the electric commutator function.

Let us now consider the two-loop causal diagrams for $\Sigma_{\mu\nu}(x,y)$, where **x**,**y** are many compton wavelengths from either boundary (the condition following eq.(2)). We also assume $|(x-y)^2| << m^{-2}$, since we are interested in the light-cone singularities of Σ. The one-loop graphs (Figs.2*a*, 2*b*) do not contribute any plate-dependent terms. At the two-loop level, there are 11 causal graphs for Σ^{****}. Figs. 2*c*, 2*d* depend on the boundaries only via the spatial range of the two internal vertex positions*****. This is because the only plate-dependent internal line is the photon retarded propagator, and there is not sufficient time for this photon to be causally reflected from a boundary in these two graphs. But spatial-range effects cannot affect the leading light-cone singularity of Σ, which comes from vertices near the light-cones of x and y.

We next turn our attention to the nine remaining two-loop graphs, shown in Figs. 3 and 4. Here, the reflection terms in the internal photon propagator do contribute. The plate-dependent piece of Σ has the following form (we again neglect spatial-range effects):

$$\Sigma^{(p)}_{\mu\nu}(x,y) = \int\int d^4z d^4w \sum_{i=1}^{2} f^{(i)}_{\alpha\beta}(z,w)\Pi^{(i)}_{\mu\nu\alpha\beta}(x,y,z,w) \tag{20}$$

where $i = 1,\ 2$ correspond to Figs. 3 and 4, respectively. Here $f^{(1)}$ is the reflection piece of the on-shell photon propagator (eq.(18)), whereas $f^{(2)}$ is the reflection piece of the retarded free photon propagator (i.e. $-\eta_{\mu\nu}$ times the reflection piece in eq.(9)).

The two functions $\Pi^{(i)}$ are separately gauge invariant. By this we mean that

$$\partial^{x\mu}\Pi^{(i)}_{\mu\nu\alpha\beta} = \partial^{y\nu}\Pi^{(i)}_{\mu\nu\alpha\beta} = 0, \tag{21}$$

and that $\Sigma^{(p)}$ is independent of the gauge of the photon propagators $f^{(i)}$. Each

**** And their charge conjugates. The charge conjugate of a causal diagram may or may not an identical diagram, but it always has the same value. Thus some of the 11 diagrams will be weighted by 2.

***** When discussing Σ, the external photon lines in these two figures are understood to be amputated.

$\Pi^{(i)}$ is a sum of one-loop graphs with four external photons. These graphs are akin to light-by-light Scattering graphs, except that the pole structure of the electron propagators is not Feynman. As in the case of the Feynman graphs, gauge invariance ensures the finiteness of $\Pi^{(i)}$ away from the light-cone.

The singularity of $\Sigma^{(p)}$ as $(x-y)^2 \to 0$ is milder than that of the corresponding plate-independent Σ, since $f^{(i)}(z,w)$ are regular at $(w-z)^2 = 0$, whereas the plate-independent photon propagators are singular. It is, in fact, straightforward to verify that $\Sigma^{(p)}(x,y)$ cannot modify the delta-function in the free commutator function (eqs. (6),(8)) by a derivative of a delta function. This is done using the position-space free propagators, especially their light-cone singularities[7] . Thus, as explained in section 3, wavefronts still move at speed c, even when the two-loop corrections to the commutator functions are taken into account.

ACKNOWLEDGEMENTS

I thank Lenny Susskind and members of the SLAC theory group for stimulating discussions.

REFERENCES

1. K. Scharnhorst, *Phys.Lett.* **B236**(1990), 354.
2. G. Barton, *Phys.Lett.* **B237**(1990), 559.
3. M. Kreuzer and K. Svozil, *Phys.Rev.***D** 34(86)1429, and references within.
4. A. Tang, *Phys.Rev.***D**, 36(87)2181.
5. Yang and Feldman, *Phys.Rev.***D** 79(50)972.
6. Bjorken and Drell, 'Relativistic Quantum Fields', McGraw-Hill, 1965; section 17.9.
7. Reference 6, Appendix C.

FIGURE CAPTIONS

Fig. 1 — The two loop vacuum-polarization Feynman graphs.

Fig. 2 — Some one- and two-loop causal graphs for the photon commutator functions. An electron or photon propagator denoted by 'r' is retarded, with the arrow pointing to the future. Likewise, 'a' denote an advanced electron propagator, with the arrow pointing into the past. A solid arrowhead denotes an on-shell propagator with the arrow pointing from y to x in eqs. (16),(17) (see text).

Fig. 3 — The six causal graphs with on-shell internal photon line. The external photon propagators are amputated.

Fig. 4 — The three causal graphs with retarded internal photon line.

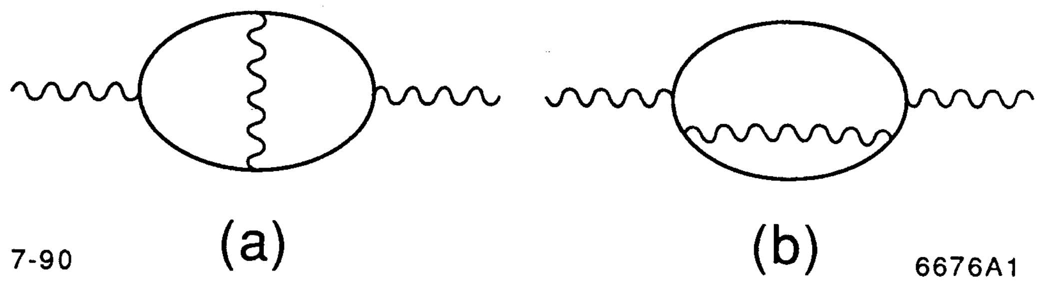

Fig. 1

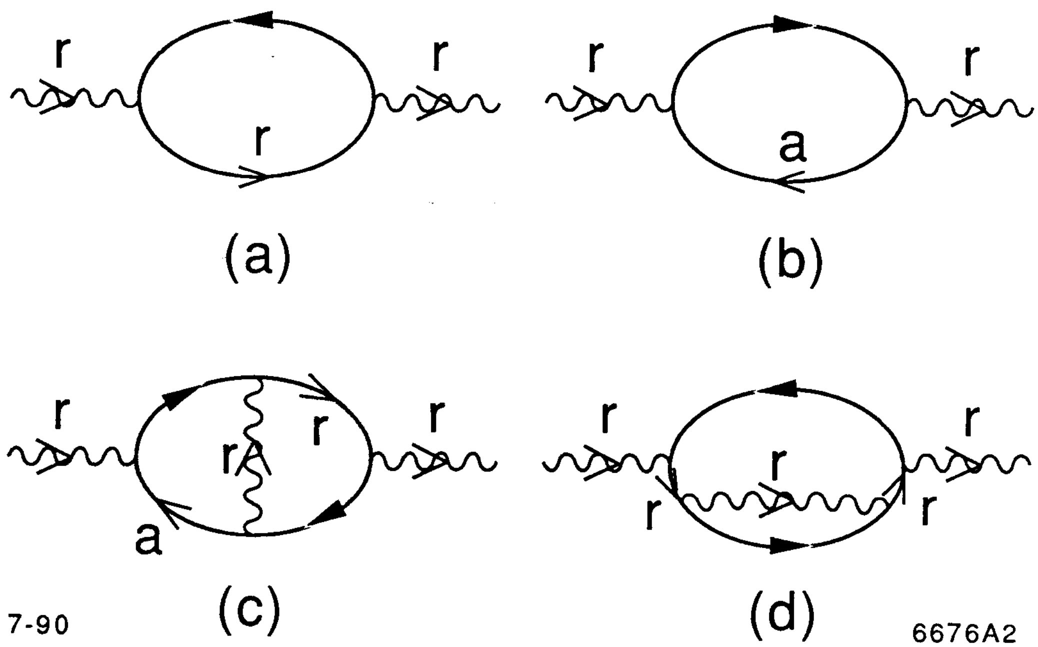

Fig. 2

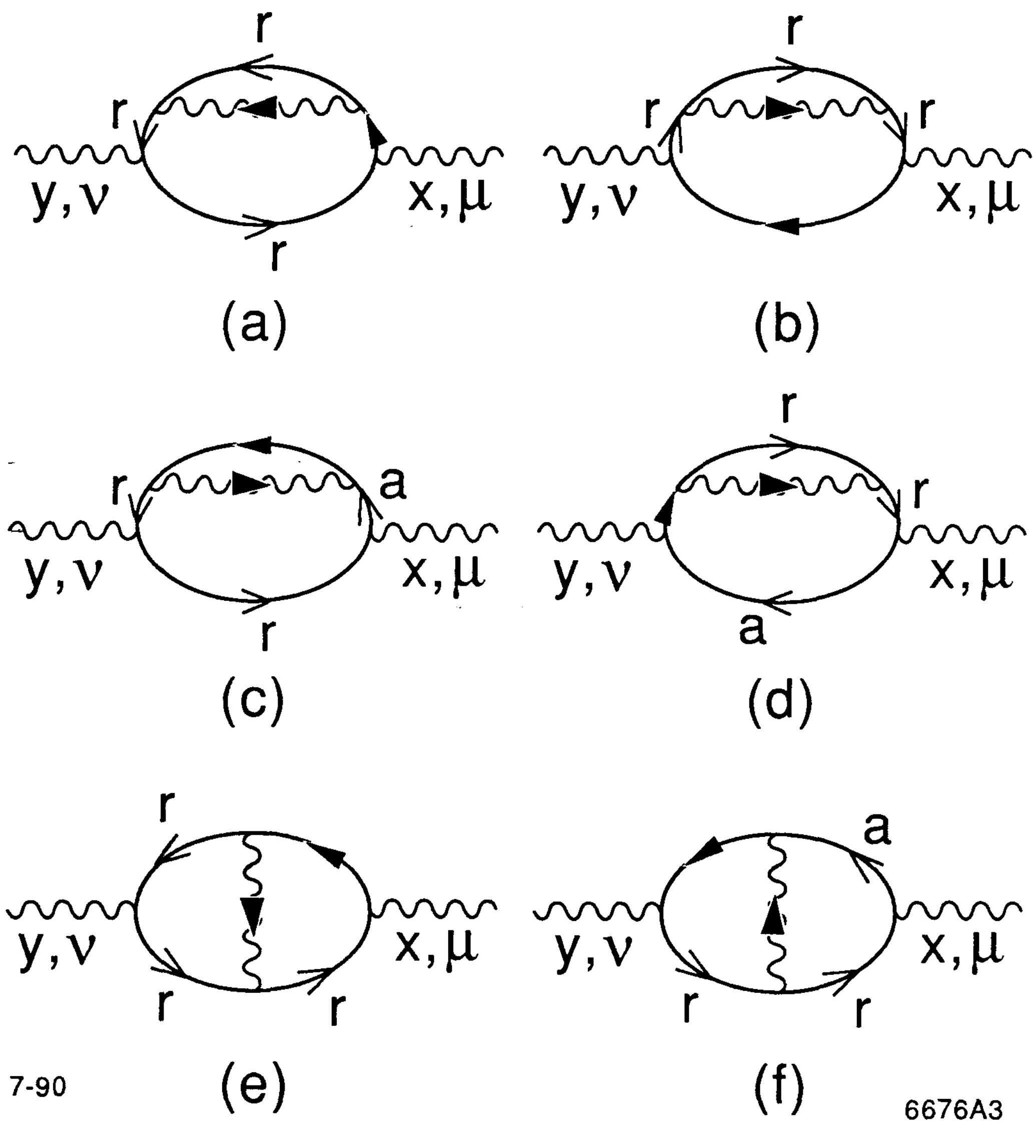
r
r
y,ν
x,μ
r
(a)
r
r
r
y,ν
x,μ
(b)
r
a
y,ν
x,μ
r
(c)
r
r
y,ν
x,μ
a
(d)
r
y,ν
x,μ
r
r
7-90
(e)
a
y,ν
x,μ
r
r
(f)
6676A3

Fig. 3

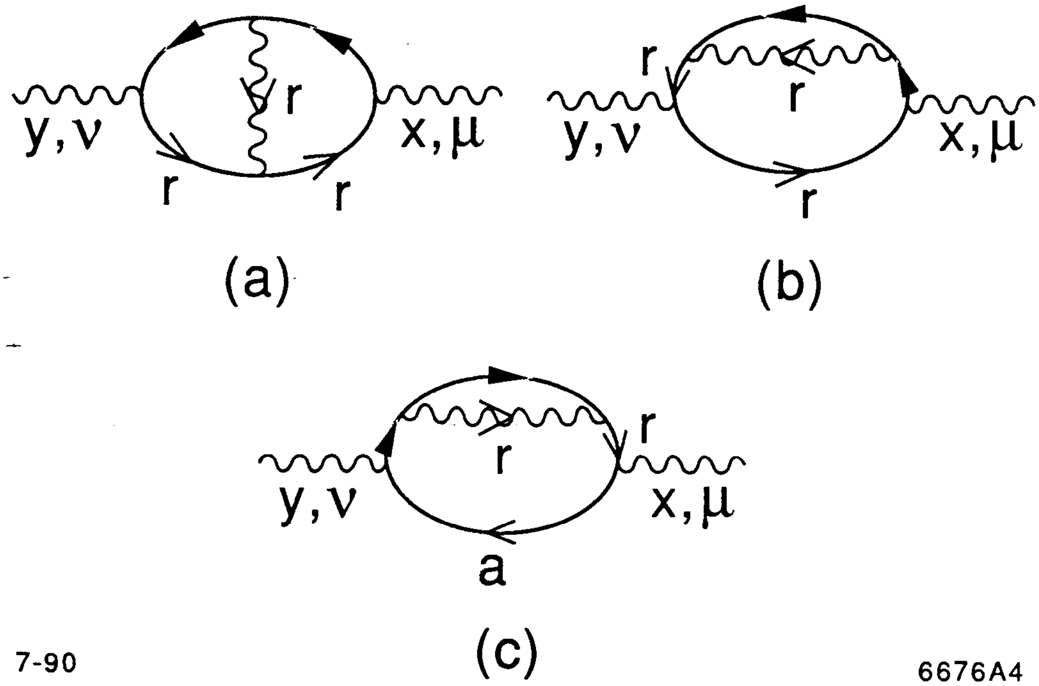

Fig. 4